Quantum chemical studies of zeolite proton catalyzed reactions

Citation for published version (APA):
Blaszkowski, S. R., & Santen, van, R. A. (1997). Quantum chemical studies of zeolite proton catalyzed reactions. *Topics in Catalysis*, *4*(1-2), 145-156. https://doi.org/10.1023/A:1019123818998

DOI:
10.1023/A:1019123818998

Document status and date:
Published: 01/01/1997

Document Version:
Publisher's PDF, also known as Version of Record (includes final page, issue and volume numbers)

Please check the document version of this publication:

• A submitted manuscript is the version of the article upon submission and before peer-review. There can be important differences between the submitted version and the official published version of record. People interested in the research are advised to contact the author for the final version of the publication, or visit the DOI to the publisher's website.
• The final author version and the galley proof are versions of the publication after peer review.
• The final published version features the final layout of the paper including the volume, issue and page numbers.

Link to publication

General rights
Copyright and moral rights for the publications made accessible in the public portal are retained by the authors and/or other copyright owners and it is a condition of accessing publications that users recognise and abide by the legal requirements associated with these rights.

- Users may download and print one copy of any publication from the public portal for the purpose of private study or research.
- You may not further distribute the material or use it for any profit-making activity or commercial gain
- You may freely distribute the URL identifying the publication in the public portal.

If the publication is distributed under the terms of Article 25fa of the Dutch Copyright Act, indicated by the "Taverne" license above, please follow below link for the End User Agreement:

www.tue.nl/taverne

Take down policy
If you believe that this document breaches copyright please contact us at:

openaccess@tue.nl

providing details and we will investigate your claim.

Download date: 24. Aug. 2022

Topics in Catalysis 4 (1997) 145–156

Quantum chemical studies of zeolite proton catalyzed reactions

S.R. Blaszkowski[1] and R.A. van Santen

Schuit Institute of Catalysis, Laboratory of Inorganic Chemistry and Catalysis / Theory Group,
Eindhoven University of Technology, PO Box 513, 5600 MB Eindhoven, The Netherlands

Theoretical chemistry applied to zeolite acid catalysis is becoming an important tool in the understanding of the adsorption and interaction of guest molecules with the zeolitic lattice. Especially the understanding of the mechanisms by which zeolite catalyzed chemical reactions proceed becomes possible. It is shown here that the old interpretation of carbonium and carbenium ions as intermediates for zeolite catalyzed reactions has to be replaced by a new approach in terms of positively charged transition states that are strongly stabilized by the zeolitic lattice. The large deprotonation energy of the acidic zeolite is overcome by stabilization of the intermediate or transition state positive charge by the negative charge left in the lattice. The zeolitic sites responsible for the adsorption and/or reaction of guest molecules are the Brønsted-acid and Lewis-base sites. We also show that different transition states are responsible for different kinds of reactions, such as cracking, dehydrogenation, etc.

Keywords: quantum chemistry; transition states; carbonium and carbenium ions; protonation reactions; acid–base catalyzed reactions

1. Introduction

Acidic zeolites catalyze a wide variety of chemical reactions making them very valuable in a variety of industrial processes. The acidic catalytic activity comes from the fact that zeolitic systems in their protonic form have a hydroxyl bridge in between an aluminum and a silicon atom, the –Al(OH)Si– group. The strength of its catalytic activity is, partially, related to the intrinsic acid strength of the proton, which is influenced by chemical composition and possibly also by the structure of the lattice, characteristic of each zeolite. Another factor that influences the reactivity of a zeolite is the stereoselectivity. Molecules that are too large to enter in the zeolite will not be converted. Also, large molecules formed inside of the zeolite microcavities that are unable to pass through the pore opening will not appear between the products.

An important feature of zeolites is their flexibility. It has been shown [1] that the flexibility of the zeolite framework is quite large and that lattice relaxation upon chemical substitutions is very important. That arises from the weakness of the Si–O–Si and Si–O–Al angle bending forces. Angles between 130° and 180° are found in natural and synthetic silicas [1] and it is exactly this flexibility that accounts for both the rich polymorphism and for the facility with which substituents, such as acidic Al–OH groups, can be accommodated in the lattice.

In the oil and petrochemical industries zeolites are largely used for processes such as cracking, isomerization and alkylations of hydrocarbons [3]. The mechanisms by which these reactions proceed involve proton transfer and formation of carbocations as reactive intermediates [3]. The details of the solid acid catalyzed reactions are now more clearly understood and appear to be quite different from liquid acid reactions. Based on mechanistic studies in superacids [4], it is proposed [3] that different carbocations can be formed, the carbonium and carbenium ions. A distinction has to be made between alkylcarbenium and alkylcarbonium ions. The first is a tri-coordinated positively charged carbon atom containing three substituents that can be alkyl groups or hydrogen atoms. Alkylcarbonium ions contain a pentacoordinated positively charged carbon atom, having the same type of substituents with the difference that at least one of the five substituents is a hydrogen atom. Below a schematic representation is shown:

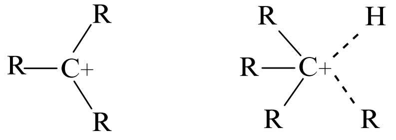

carbenium carbonium

where R = H or alkyl group.

Those carbocations can occur according to different mechanisms. The protonation of an alkene (olefin) leads to the formation of an alkylcarbenium ion. If the proton is added to a saturated molecule such as an alkane (paraffin), the protonation leads to the formation of an alkylcarbonium ion. This ion can also be transformed into a smaller alkylcarbenium ion by abstraction of an electroneutral molecule (an alkane or molecular hydrogen), involving explicitly cracking reactions. The activation of an alkane is more difficult than an alkene and occurs under high temperature conditions.

The carbocations involved in the zeolite catalyzed

---

[1] To whom correspondence should be addressed.

reactions, in contrast to those on homogeneous medium, do not occur as stable intermediates but are (part of) transition states stabilized by the interaction with the acidic and basic sites of the zeolitic lattice [5]. The stabilization effects provided by the negatively charged wall are rather strong and are necessary in order to overcome the high energy cost of the heterolytic OH dissociation. In zeolites carbonium ions are not stable ions but transition states, often with very different configurations from the corresponding carbonium ions in the gas phase [6]. Carbenium ions are found as fragments of the carbocation transition structures. In the ground state, the carbenium ion fragments are converted to alkoxy species. For their existence there is NMR spectroscopic evidence [7].

The following points will be extensively discussed here:

– the mechanism of protonation reactions where both the Lewis-base and the Brønsted-acid sites are involved;

– carbonium and carbenium ions as (part of) transition states responsible for different reactions and their relative stability;

– the selectivity between the type of the reaction versus kind of transition state formed;

– acidity dependence of the zeolitic structure and influence over activation barriers;

– mechanistic study of zeolite catalyzed reactions according to an associative versus an alkoxy mediated mechanism.

2. Lewis-base and the Brønsted-acid catalyzed reactions

As reported by Kramer and van Santen [5], the deprotonation energies or proton affinity, PA (the energy necessary for the removal of one proton), of an acidic zeolite are in the order of 1250 kJ/mol. This is very large in comparison to experimental activation barriers for zeolite catalyzed reactions such as hydrogen-exchange, dehydrogenation or cracking of, for example, *n*-butane that involve true barriers not higher than 200 kJ/mol [8] or dehydrogenation of methane, where the activation barrier was calculated to be ~ 350 kJ/mol [9]. The explanation for this large difference is that in a zeolitic system, when a proton is transferred to a guest molecule, there will be a compensation between the negative charge left in the lattice and the positive charge created in the molecule. The PA differences between the various types of zeolite oxygens that are deprotonated give valuable information about where the proton will preferably sit in the zeolitic lattice. For example, Kramer and van Santen [10] observed that for MFI (HZSM5) oxygen sites that are part of the 10-membered rings, that surround the MFI channels, are less favorable for proton attachment than oxygen sites that are no part of one of the 10-rings. For faujasite there is an excellent agreement between theoretically predicted and experimentally observed occupied sites [10].

As discussed above, in zeolitic systems the proton is initially strongly bonded to the lattice. In order to overcome this large deprotonation energy, the protonated guest molecule has to be stabilized by the negatively charged lattice. The interaction takes place with two (or three) adjacent oxygen sites, the Brønsted-acid site and the corresponding Lewis-base sites. Fig. 1 shows this for three different modes of interaction of methanol and water with the zeolite cluster model. In the first mode (fig. 1a) the structure of the hydrogen bonded adsorption complex of one methanol molecule is shown. The methanol hydroxyl group is directed to the surface while methyl is directed into the cavity. The oxygen of the methanol hydroxyl group interacts (is hydrogen bonded) with the zeolitic proton, the Brønsted-acid site, which remains covalently bonded to the zeolite, while the hydrogen atom of the hydroxyl group interacts with a basic lattice oxygen, the Lewis-base site. Fig. 1b shows the transition state (TS) for the reaction of hydrogen exchange of methanol. The Brønsted-acid / Lewis-base sites interaction is similar as in fig. 1a except that now

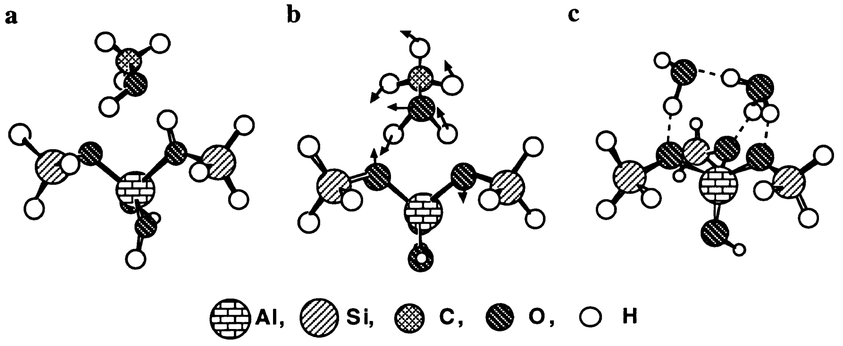

Fig. 1. (a) Adsorption complex for one methanol molecule, (b) transition state for the reaction of hydrogen exchange of methanol (the arrows represent the displacement of the atoms according to the only imaginary mode, the reaction coordinate) and (c) complex of adsorption of two water molecules. All structures were obtained at the DFT/DZVP including Becke and Perdew nonlocal corrections selfconsistently. (Pictures (a) and (b) are reprinted from ref. [12], copyright 1995 American Chemical Society; and (c) from ref. [14].)

the zeolitic proton has been partially transferred to the methanol. This reaction is very fast with an activation barrier calculated to be not higher than 12 kJ/mol according to different methods, basis sets and zeolite cluster models used [11–13]. Additionally with two adsorbed molecules, a three-center interaction can occur, one at the Brønsted-acid site and the other two at the Lewis (or Brønsted)-base sites. This kind of interaction can be seen in fig. 1c, where two water molecules are shown to adsorb at the zeolitic surface [14]. Whereas the proton would not transfer for adsorption of one single H_2O molecule [15] at higher water coverages (fig. 1c), the zeolitic proton is observed to be transferred to one of the water molecules without any activation barrier [14–16]. In this case a hydronium intermediate stabilized by the additional water molecule is formed.

The examples above show that in zeolites the molecules adsorb and react in “reaction steps” that involve the Brønsted-acid as well as the Lewis-base sites. Thus, the cluster choice is very important to correctly represent the system studied. For instance, a cluster that contains only the acidic site ($H_3Si(OH)AlH_3$) is not able to represent reactions that are acid–base catalyzed. In ref. [17] is proposed that the protolytic cracking of butane was not driven by an acidic–base pair type reaction, while others [18–20] propose exactly the opposite. The reason for ref. [17] to find that cracking is not an acid–base catalyzed reaction is due to the use of a physically incorrect cluster. Another example is the adsorption complex of fig. 1c. A cluster that has only hydrides terminating the aluminum atom, the $H_3SiOAlH_2(OH)SiH_3$ cluster, would not be suitable to correctly represent the three-fold interaction of the right-side water molecule. The use of the larger $H_3SiOAl(OH)_2(OH)SiH_3$ cluster, although it contains a second basic site (one of the OH terminations of the aluminum atom), would also be inadequate because of the difference in physical environment of each of the basic sites.

3. Carbonium and carbenium ions versus transition states and their relative stability

Not long ago, the first indications [21–23] that the traditional interpretation of carbenium and carbonium ions as intermediates for zeolite catalyzed reactions has to be reconsidered were given. The old view on the existence of protonated intermediates has to be replaced by a new interpretation in terms of transition state structures adsorbed on the zeolitic lattice. Each reaction mode proceeds via a different transition state. In homogeneous superacid catalyzed reactions, the activation of alkanes proceeds via carbonium ions and, in the case of cracking and dehydrogenation reactions, a carbenium ion will be generated in a consecutive step. Alkene activation proceeds directly to a carbenium ion. In homogeneous superacid catalyzed reactions, two factors are different from those in heterogeneous zeolite catalyzed reactions. First, as discussed in the previous section, the energy for deprotonation of the zeolite is considerably higher than in superacid catalysts. This induces the activation barriers for zeolite catalyzed reactions to become also much higher. Second, in contrast to the homogeneous medium, the solvation effects are absent in the zeolites [4]. This will require carbonium and carbenium ion intermediates to be stabilized by the zeolite negative lattice.

Although sometimes the geometry and charge distribution of the carbonium-like transition structures may resemble that of the free ions, they cannot really be considered as free species, because of their strong electrostatic interaction with the surface. The carbonium-like transition states derive from the direct protonation of the organic molecule by the acidic zeolite and are not stable structures, but correspond to a maximum in the potential energy surface. Examples for this kind of transition structure are depicted in figs. 2a and 2b. In fig. 2a the transition state for the hydrogen exchange reaction of ethane, analogous to the transition state for hydrogen exchange of methanol (fig. 1b), is shown. In this TS one of the carbon atoms has been protonated by the zeolite becoming then penta-coordinated, while the second carbon atom maintains clearly its tetrahedral geometry. Although the geometry of this structure is very similar to that of a free carbonium ion, its Mulliken charges are different, as can be observed from table 1. The $C_2H_7^+$ group can be divided into two distinct parts: the C_2H_5, nearly neutral, and the two hydrogens in between the carbon and the two hydrogens, which are positively charged. These structures are different from the corresponding carbonium ions measured by mass spectroscopy [24] or computed by ab initio calculations [6] for free methyl carbonium ions, which are found to consist of a complex between methyl carbenium ion plus a molecular hydrogen.

In fig. 2b one of the two possible transition states for ethane cracking is shown. The zeolitic proton has been transferred to the right-side carbon of the ethane molecule and one hydrogen of the right-side carbon has moved in between both carbons. This is an example of a three-center two-electron bond (atoms C1, C2, and H2 in fig. 2b). The same structure could also be characterized as an almost formed methane in the right-side interacting with a carbenium ion (CH_3^+) in the left side, which is stabilized by the basic oxygen of the lattice (see table 1).

Carbonium type transition states can often be decomposed in a carbenium ion part and a neutral molecule. The local geometry around the positive tri-coordinated carbon atom is, in general, close to that of the free carbenium ion. An example is shown in fig. 2c. The carbon atom C1 has a hybridization very close to sp^2 and a geometry close to trigonal planar, exactly as the one found in free carbenium ions. They are also positively charged as in free carbenium ions. Together with the

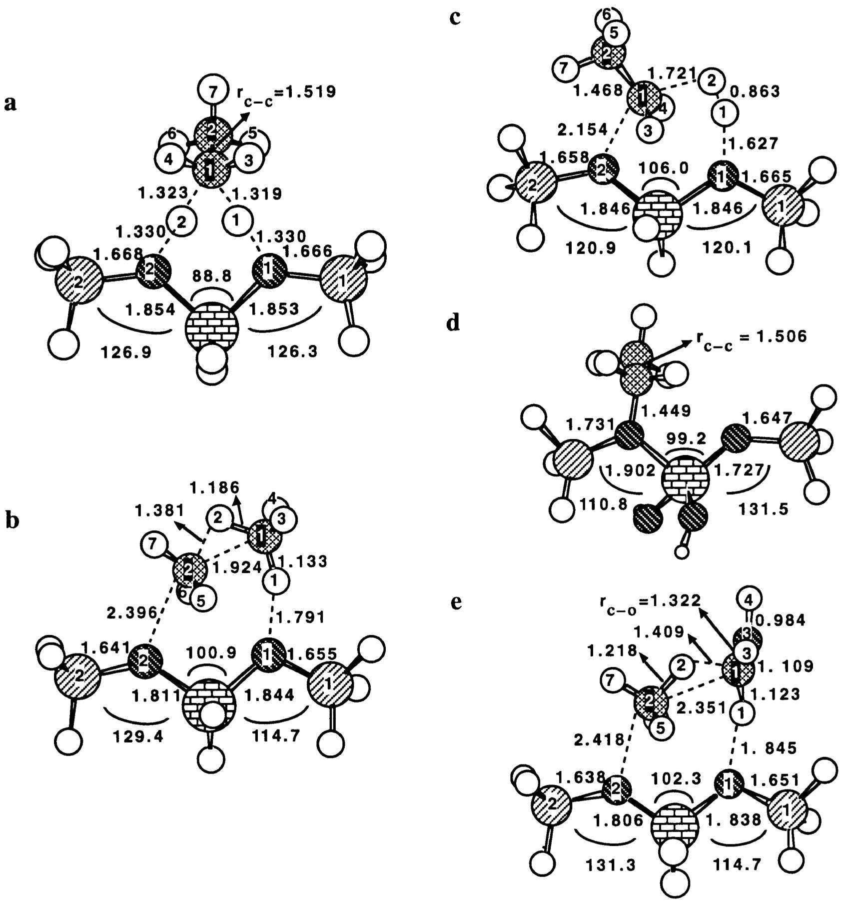

Fig. 2. Transition states for (a) hydrogen exchange, (b) cracking, and (c) dehydrogenation of ethane, (d) surface ethoxy species and (e) TS for hydride transfer between methanol and a surface methoxy species. All structures were obtained with DFT/DZVP including nonlocal corrections at the end of the optimization. Distances in Å and angles in deg. See fig. 1 for the pattern of the atoms. (The pictures (a)–(c) and (e) are reprinted from ref. [19], copyright 1996 American Chemical Society.)

almost formed H_2 "molecule", they form a complex TS for the dehydrogenation reaction of ethane [19]. In the ground state, those carbenium-like transition structures react to form surface alkoxy species.

Via the transition state shown in fig. 2c the $C_2H_5^+$ group reacts with the surface forming a surface ethoxy species, shown in fig. 2d. The alkoxy groups are the only stable form (ground state) of a carbenium-like ion found in zeolitic systems. After formation, those surface alkoxy species can undergo chemical reactions. One of the reactions is the hydride transfer reaction. The TS for the formation of a methane molecule from a surface methoxy plus methanol via a hydride transfer reaction [19] is shown in fig. 2e. The $C(OH)H_2$ group generated now binds to the surface. In a consecutive step, one of the hydrogen atoms that was bonded to the carbon atom is transferred to the zeolitic surface regenerating the acidic site and, simultaneously, a formaldehyde molecule will be desorbed. This is consistent with experimental evidence for such a reaction [25]. In general, hydride transfer reactions proceed via a lower activation barrier than the reactions that involve carbenium ion transition states, such as cracking and dehydrogenation. The hydride transfer reaction between a methane molecule and a surface methoxy species, according to Hartree–Fock (HF) calculations performed by Kazansky et al. [20,26], involves an activation barrier of 256 kJ/mol, which is 60–75 kJ/mol lower than the cracking (315 kJ/

Table 1
Mulliken charges of some atoms for the transition states of ethane hydrogen exchange, cracking and dehydrogenation (figs. 2a, 2b and 2c, respectively)

	C1	C2	H1	H2	H3	H4	H5	H6	H7
hydrogen exchange	−0.657	−0.670	0.294	0.294	0.276	0.272	0.246	0.246	0.247
cracking	−0.792	−0.744	0.339	0.315	0.303	0.304	0.355	0.366	0.313
dehydrogenation	−0.511	−0.640	0.149	0.050	0.352	0.379	0.269	0.267	0.248

mol) and dehydrogenation (333 kJ/mol) of ethane obtained by the same authors [20].

The reaction activation barriers depend on the relative stability of the carbenium ion transition states. This varies with the primary, secondary or tertiary nature of the carbon atom, center of the ion's positive charge. According to DFT/DZVP calculations including nonlocal corrections [9], the relative stability of different free carbenium ions with respect to the gas phase neutral molecules is (in kJ/mol):

$$\mathrm{H_3C^+} \ll (199)\ \mathrm{CH_3H_2C^+} < (96)\ \mathrm{(CH_3)_2HC^+} < (66)\ \mathrm{(CH_3)_3C^+}\,.$$

The single CH_3^+ is much less stable than the other carbenium ions. Based on these values, one would expect that the activation barrier for different reactions will also depend on the stability of the carbenium-like transition structure formed. Table 2 shows calculated activation barriers with respect to the gas phase reactants of different acid zeolite catalyzed reactions of some saturated hydrocarbons. The activation barrier for the reaction of hydrogen exchange almost does not change on going from the CH_5^+ to the $C_2H_7^+$ carbonium ion, indicating no intermediate CH_3^+ or $C_2H_5^+$ formation. For cracking and dehydrogenation, where carbenium-like transition state structures are involved, the inclusion of additional carbon atoms has a strong stabilization effect. The DFT results [9,19] for the dehydrogenation reaction show a stabilization of almost 50 kJ/mol on going from the single CH_3^+ to the $CH_3H_2C^+$ carbenium-like transition state that are involved in the activation of methane and ethane, respectively. The MP2/6-31++G**//HF/6-31G* activation barrier obtained by Kazansky et al. [27] for the dehydrogenation of ethane, where a primary carbenium ion is involved (333 kJ/mol), shows an stabilization of 50 kJ/mol for isobutane dehydrogenation (279 kJ/mol) that occurs via a tertiary carbenium-like TS [28].

These results enable us to conclude that the dehydrogenation barrier for isobutane is ~100 kJ/mol lower than for methane. According to the scheme shown above, the CH_3^+ carbenium ion is ~350 kJ/mol less stable than the larger $(CH_3)_3C^+$ ion. The reason why methane dehydrogenation does not require 350 kJ/mol more than isobutane but only 100 kJ/mol is the fact that the carbenium ion transition state formed is also stabilized by the zeolitic surface. The CH_3^+ type carbenium-like ion is more stabilized by the surface than $(CH_3)_3C^+$. The same behavior is also observed for the cracking reaction, except that the stabilization effects are larger, over 70 kJ/mol [20,28] on going from the cracking of ethane to isobutane.

The conclusion is that the cracking reaction of isobutane, where a secondary carbenium ion is formed, should be easier (lower activation barrier) than the cracking of *n*-butane or propane, where a primary carbenium ion will be formed. The same analogy can be made for the dehydrogenation reaction, except that now for isobutane a tertiary or a primary carbenium-like TS will be formed and for *n*-butane a secondary or primary carbenium-like will be formed. Those previsions seem to be somewhat controversial if one compares the experimental dehydrogenation and cracking apparent activation barriers obtained for *n*-butane using a HZSM5 zeolite [31], respectively 149 and 140 kJ/mol, with those for isobutane for a highly dealuminated USY zeolite [32], 165 and 157 kJ/mol, as shown in table 2. The reasons for the difference in the experimental activation barriers for *n*- and isobutane are due to the differences in the heat of adsorption for different zeolites. Bates et al. [33] have shown that the heat of adsorption for different zeolites

Table 2
Activation barriers (in kJ/mol) for different zeolite catalyzed reactions of some alkanes

	Font	Ref.	Hyd. exchange	Cracking	Dehydrogen.	Hyd. transfer
methane	exp.	[5,22][a]	130	–	–	–
	DFT	[9]	120	–	345	–
	HF	[26,27]	155	–	437	278[e]
	HF	[22,29]; [30]	150 ± 20; 154	–	–	–
ethane	DFT	[19]	118	292	297	–
	HF	[18,27,20,26]	–	391[c], 315[d]	397[c], 333[d]	236[f]
n-butane	exp.	[8][a]	85	140	105	–
	exp.	[31][a]	–	140	149	–
isobutane	exp.	[32][b]	–	157 ± 20	165 ± 20	< 167
	HF	[20,28,26]	–	241[d]	279[d]	202[g]

[a] HZSM5, Si/Al = 35.

[b] USY, Si/Al = 172.

[c] HF/3-21G and partial optimization.

[d] Energy at MP2/6-31++G**//optimization at HF/6-31G*.

[e] With respect to methane plus a surface methoxy species.

[f] With respect to ethane plus a surface ethoxy species.

[g] With respect to isobutane plus a surface *t*-butoxy species.

increases with the decrease in pore size of the zeolite. For a first-order reaction the apparent activation energy is given by the true activation energy minus the adsorption energy ($E_{\text{bar(app)}} = E_{\text{bar(true)}} - E_{\text{ads}}$). For zeolites with the same intrinsic acidity, the $E_{\text{bar(true)}}$ for a specific reaction has been observed to be constant [34]. From that one concludes that for the same reaction, larger apparent activation barriers will be measured for a USY zeolite than for a HZSM5. This becomes clear in the scheme shown in fig. 3. The fact that isobutane activation has a lower activation barrier than *n*-butane is less important than the adsorption energy effects, as can be concluded from the experimental apparent activation barriers (table 2).

According to HF calculations [20,28], the apparent activation barrier for isobutane cracking is 240 kJ/mol while for dehydrogenation it is 280 kJ/mol (see table 2). Those barriers are approximately 100 kJ/mol higher than the respective experimental apparent barriers. Since butane is a relatively large molecule, it will interact not only at the Brønsted-acid and Lewis-base sites, but also with the next-near-neighbor atoms of those sites. This will result in an extra stabilization that will help the apparent activation barrier to decrease. The difference between true and apparent activation energy is much less for small molecules as methane or ethane. The small $Al(OH)_3OH_2$ cluster used by Kazansky [20,28] is much too small and does not allow for the extra stabilization of the molecule. This is probably the reason for the much higher calculated activation barriers compared to the experimental values (table 2) as well as adsorption heats that are just slightly exothermic. Because of that, the computed activation energies in this case should be compared to the experimental true activation energies.

4. Type of reaction versus kind of transition state

Each chemical reaction proceeds via a characteristic transition state intermediate. One specific chemical reaction goes through a geometrically analogous transition state for different compounds. For example, the TS involved in the reaction of hydrogen exchange of methanol (fig. 1b) has the same characteristics as the carbonium-like TS for the hydrogen exchange reaction of methane (not shown), ethane (fig. 2a) as well as benzene [35], shown in fig. 4a. In order to accommodate the proton coming from the zeolite, the reactant molecule has to deform. Calculations show [9,19,27,29,30,35] that the carbonium-like structures do not correspond to a minimum in the potential energy surface but to one of the degrees of freedom, the reaction coordinate; they are a saddle point (maximum point) which is characterized by the presence of an imaginary frequency. An analysis of the displacement of the atoms along such imaginary mode shows which products are formed, or, when followed in the opposite direction, shows the reactants. An example is shown in fig. 1b, the TS for hydrogen exchange of methanol. The arrows represent the displacement of the atoms along the only imaginary mode, which is the transfer of the zeolitic proton to methanol and the symmetrical return of the hydrogen atom from methanol to the zeolite. The carbonium ion formed is, thus, not a stable intermediate, but has to be considered a transition state. The interaction of the carbonium ion with the zeolite is more covalent than ionic, as can be observed from the short distances between the carbonium ion and the lattice atoms shown in table 3.

The hydrogen exchange TS is very different from transition states involved in other reactions like dehydrogenation and cracking, as shown for ethane in fig. 2b and 2c. While in the TS for hydrogen exchange the Lewis-basic oxygen of the lattice stabilizes a hydrogen atom of the adsorbed molecule (H2 atom on fig. 2a – H1 is assumed to be the zeolitic proton), in the TS for dehydrogenation and cracking it will compensate the positive charge generated in the RH_2C^+ carbenium-like part of the transition structure. With respect to the transition

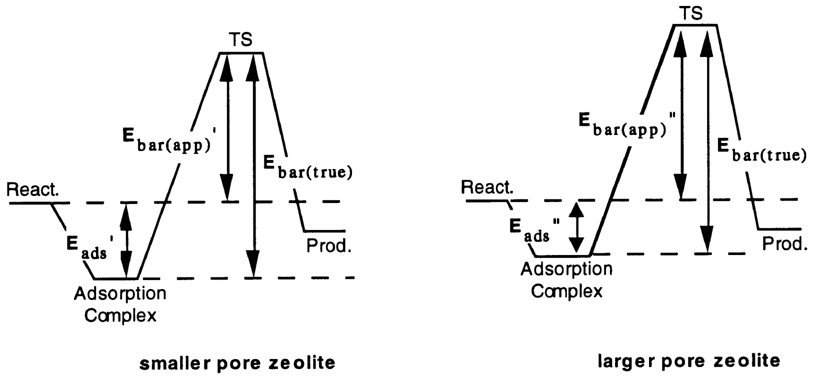

smaller pore zeolite **larger pore zeolite**

$$E_{\text{ads}}' + E_{\text{bar(app)}}' = E_{\text{ads}}'' + E_{\text{bar(app)}}'' = E_{\text{bar(true)}}$$

Fig. 3. The relation between the apparent activation energy, $E_{\text{bar(app)}}$, and the adsorption energy of the molecule, E_{ads}, for a first-order reaction of two different zeolites with same intrinsic acidity.

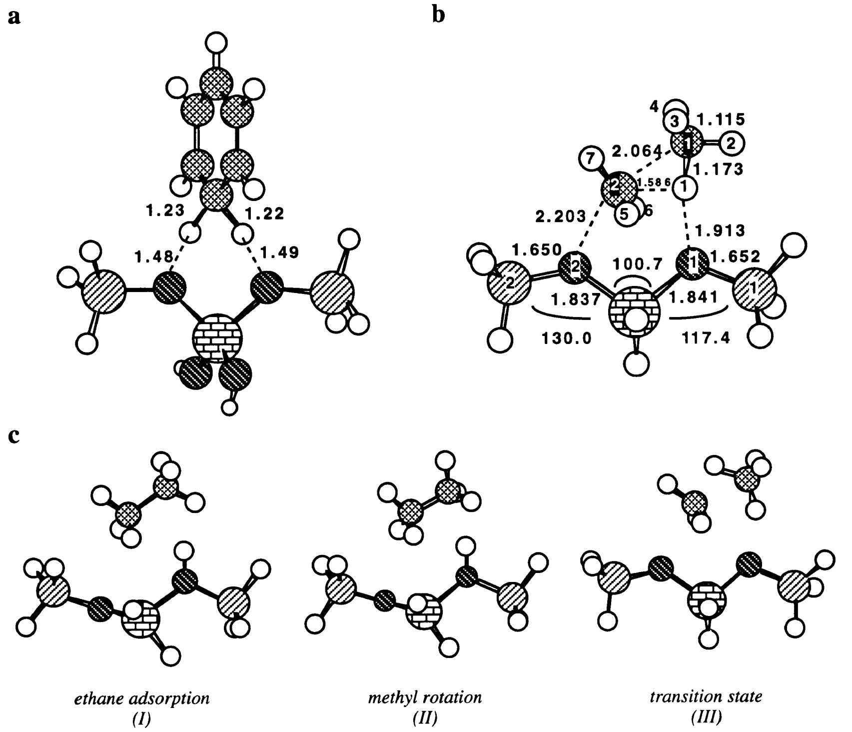

ethane adsorption *(I)*

methyl rotation *(II)*

transition state *(III)*

Fig. 4. Transition states for (a) hydrogen exchange reaction of benzene, (b) one step and (c) three steps ethane cracking reaction. Distances in Å and angles in degree. See fig. 1 for the pattern of the atoms. (Picture (a) is reprinted from ref. [35] and (b) and (c) from ref. [19]. Copyrights 1995 and 1996 American Chemical Society.)

states for dehydrogenation (fig. 2c) and cracking (fig. 2b), the basic difference is that in the first the zeolitic proton attacks a C–H bond, while in the second, a C–C bond is attacked.

Sometimes, different paths are observed for a specific chemical reaction involving, thus, distinct transition states for each path. An example is the ethane cracking reaction, that can occur in one step involving the TS shown in fig. 4b or can proceed in more than one step, requiring the rotation of one of the methyl groups, as shown in fig. 4c. The activation barrier involved is exactly the same for both TS.

The last topic to address refers to the fact that chemical reactions proceed via several different adsorption steps, involving, thus, the formation of several different structures (TS's and adsorption complexes) along the reaction path. This is due to the many different configurations that an adsorbed molecule can take with respect to the surface. An example of this kind of reaction is the dehydration of methanol with formation of surface methoxy species, as presented in fig. 5. A single methanol molecule can adsorb at the acidic site of a zeolite according to two different modes, end-on and side-on. In the first, methanol adsorbs perpendicular to the surface with the hydroxyl group interacting with the zeolitic proton. This is the most stable mode of adsorption, as shown in

Table 3
Selected distances (in Å) of the hydrogen exchange TS's for different compounds and methods

	DFT				HF		
	methanol [12]	benzene [35]	ethane [19]	methane [9]	 [22,29][b]	methane [30][c]	 [27][d]
O–H	1.12	1.23	1.32	1.31	1.28	1.16	1.15
C–H	1.35[a]	1.48	1.33	1.34	1.40	1.50	1.53
Al–O	1.86	1.81	1.85	1.82	1.80	1.86	1.83
Si–O	1.69	–	1.67	1.67	1.65	–	–

[a] For methanol, instead C read O.
[b] 3T atoms cluster and 6-31G** basis set.
[c] 1T atom cluster and 6-31+ +G** basis set.
[d] 1T atom cluster and 3-21G basis set.

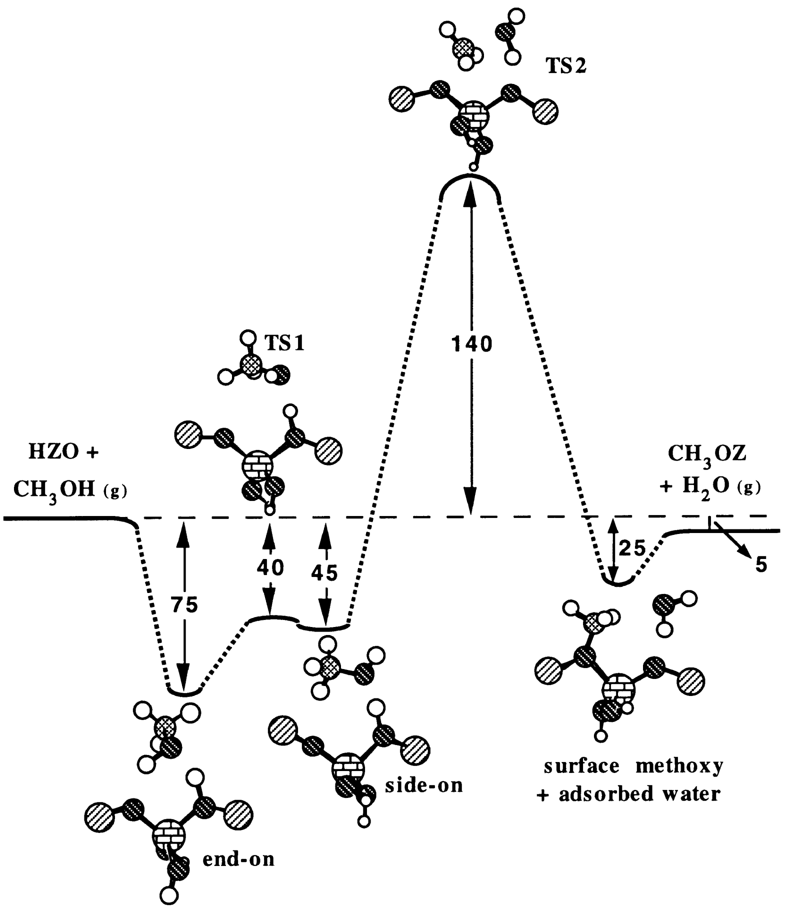

Fig. 5. Reaction energy diagram for methanol dehydration with formation of surface methoxy species (kJ/mol). The hydride termination of the Si atoms is, for clarity, not shown. See fig. 1 for the pattern of the atoms.

fig. 5. Via TS1 (shown in the figure), methanol rotates until the next adsorption complex, side-on. In this new mode of adsorption, methanol becomes parallel to the surface and the C–H group of methanol is directed to the basic oxygen of the zeolite while the oxygen of methanol is directed to the zeolitic proton. In this configuration the hydrogen of methanol's hydroxyl group is directed to the cavity. Now methanol has a good conformation with respect to the surface and, via the transition state TS2, can dehydrate generating also a surface methoxy group.

5. Acidity effects

Kramer and van Santen [22,29] have shown how the proton affinity (the theoretical measurement of the zeolite acidity) can be modified by chemical and structural variations in the zeolitic lattice. The proton affinity can be mimicked by constraining the peripheral bonds of the zeolite cluster. By assigning different bond lengths to the terminal Si–H bonds of the cluster and optimizing all other parameters, the proton affinity varies over a range of 1–2 eV, which is the same magnitude as the expected variation in real zeolites. Fig. 4 shows the general effect of changing the peripheral Si–H distances for the zeolite cluster. On making the Si–H's longer, the Si–O bond becomes shorter, and, as a consequence, O–proton longer. In other words, the bond O–H becomes weaker, and the zeolite more acidic. Making Si–H bonds shorter represents making the zeolite cluster less acidic. If the Si–H bonds in the left side of the cluster are changed instead, the effect is nearly the same, but now it is of "long distance", and so, weaker. Changes in the acidity of the cluster provoke also changes in the activation barrier or adsorption energies, as observed experimentally [32,34] for different zeolites. To change the Si–H bonds in the transition state structures will provoke a different response according to their nature, more covalent or ionic. The alternation in the bond distances due to the change in Si–H bond length are in agreement with bond order conservation (BOC) arguments [36].

Table 4 shows the effect that changes in the proton affinity of the zeolite have on the activation barriers of a few reactions of ethane [19]. Shortening the Si–H distances in the TS for the hydrogen exchange reaction (fig. 2a) in one side by approximately 0.2 Å, which means making the zeolitic site less acidic by decreasing the bond

Table 4
Effect of changes in the Si–H distances of transition states of different reactions over their activation barriers (in kJ/mol). S = shorter and L = longer. Follow also figs. 2a, 2b and 2c

	Equilibrium	Left S	Left L	Right S	Right L	Left/right S	Left/right L
hydrogen exchange	118	132	115	132	115	125	122
cracking	292	301	295	312	283	310	280
dehydrogenation	297	303	303	314	291	311	291

strength of zeolite–proton, the activation barrier is found to increase to 132 kJ/mol. A lengthening of the Si–H distances by ~0.2 Å results in the weakening of the O–H bond and a decrease in the activation barrier to 115 kJ/mol. Changes in the Si–H bond lengths on the right hand side have a similar effect as changes in the left hand side, due to the symmetrical characteristic of this transition state. When the Si–H's in both sides are made longer or shorter simultaneously, there is compensating change in the relative energies, as can be seen from the small increase in the activation barrier for both cases (longer and shorter). This is due to the covalent nature of the transition state. The energy barrier depends on the difference in proton affinity of O1 and O2. Exactly the same trend was also observed by Kramer and van Santen for methane hydrogen exchange [22,29].

The effect of changing the distances of the terminal Si–H bonds on the reactions of cracking (fig. 2b) or dehydrogenation (fig. 2c) is nearly the same, but very different than it was for hydrogen exchange. The change in behavior is due to the dominance of the ionic contributions to the interaction energy. When the interaction is purely ionic, the stabilization of the cation only depends on the oxygen charges and, thus, is not significantly affected by changes in Si–H bonds. In agreement with this, the dominating parameter that now controls the activation barrier is the bond energy of the proton in its ground state. Changes in the left-side Si–H bonds almost do not affect the activation barrier, but only in the right-side. The increasing acidity (longer zeolite–proton distance or, in other words, lower proton bond energy) reduces the activation barrier for dehydrogenation reaction less than for cracking, implying that the transition state for cracking is more ionic.

For systems where a medium to strong base (like methanol or acetonitrile) is being adsorbed at the zeolite system, acidity effects are very important. For instance, when methanol is physisorbed (hydrogen bonded) at the acidic site of a zeolite at low coverages (one molecule per acidic site), the ground state adsorption complex is observed not to be protonated [12,14]. The corresponding protonated species has been found [11–13] to be a transition state. Very recently, results of a periodic system calculation using a plane-wave basis set reported [37] that when methanol is situated in the eight-ring window of a chabazite zeolite, protonation occurs without any activation barrier. If, nevertheless, the methanol is located inside of a more open cage region, such as those found in sodalite, only hydrogen bonded (physisorbed) methanol is observed. In this stage it is not clear whether these results can be considered as proof that channel electrostatic effects are important or that local geometric effects could better explain these results.

When the right-side Si–H distances of the structure shown in fig. 1a are made longer, representing thus a more acidic zeolite, no protonation is observed. When methanol is adsorbed at higher coverages, for instance two methanol molecules per acidic site, the ground state is also observed not to be protonated [14], but remains hydrogen bonded adsorbed, as shown in fig. 6b (I). When such adsorption mode is made more acidic by making the Si–H distances close the O–proton longer by 0.2–0.3 Å the zeolitic proton is observed to migrate to one of the methanol molecules [14], as shown in the scheme of fig. 6b (II and III). The adsorption energy is also observed to decrease, also shown in fig. 6b. This suggests that for a very acidic zeolite, methanol adsorbed at high coverages can possibly be observed also in its protonated form.

Recently it has been observed [38] that, if two methanol molecules are adsorbed at a SAPO type zeolite, the proton is transferred to one of the methanol molecules assuming an analogous configuration as for alumino-silicate shown in fig. 6b (I). This is somewhat surprising, since a SAPO is less acidic than an alumino-silicate. The protonation would not be expected. The reason for this result is that the molecular system used to represent the SAPO zeolite, the $H_3Si–OH–Al(OH)_2–O–PH_3$ cluster, does not represent a neutral system. On replacing a Si atom (+4) by a P (+5), the resulting charge is +1. To make the system neutral, the proton cannot be included. The smallest neutrally charged AlPO clusters containing a proton are represented schematically by:

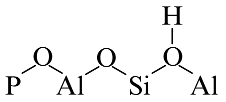

and

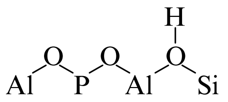

which illustrates the importance of a proper choice of cluster models for the zeolite.

A large effort is being done in order to understand the relation between the zeolite structure and its reactivity [39–41]. An important item to address now is the zeolite acidity dependence on cluster size. Brand et al. [39] have shown that the inclusion of a shell of oxygens increases the zeolite proton affinity, whereas the inclu-

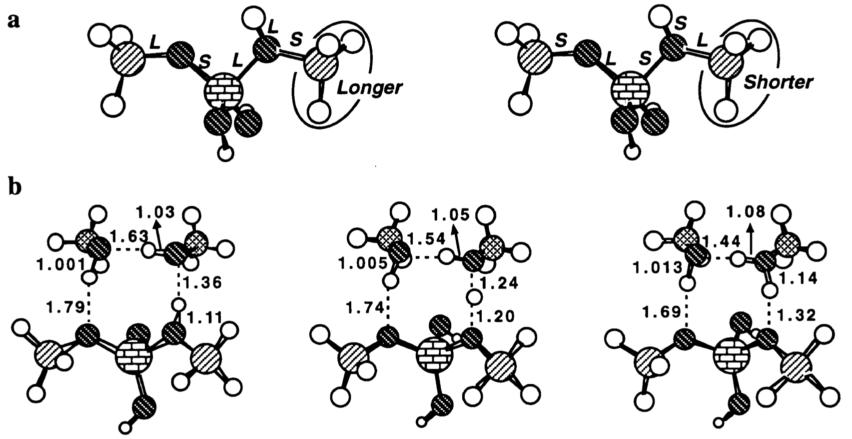

Si-H (r) equilibrium
E_{ads} = -139 kJ/mol
(I)

Si-H (r) long
E_{ads} = -142 kJ/mol
(II)

Si-H (r) very long
E_{ads} = -145 kJ/mol
(III)

Fig. 6. (a) Change in the bond distances of a 3T atoms cluster according to changes in the Si–H bond distances (S= shorter, L = longer) and (b) representation of the ground state adsorption complex of two methanol molecules with the right-side (r) Si–H bond distances at the (I) equilibrium, (II) equilibrium +0.2 Å, and (III) equilibrium +0.3 Å, together with the respective adsorption energies (ZPE corrections are not included). The Si–H bond distances in the left-side are always in the equilibrium. Distances in Å. See fig. 1 for the pattern of the atoms. (Picture (a) is reprinted from ref. [19], copyright 1996 American Chemical Society.)

sion of a new silicon shell decreases it. According to DFT calculations the PA for an 8T atoms cluster (T = Si, Al) is in the order of 1340 kJ/mol [40] while for the commonly used 3T atoms cluster it is 1260 kJ/mol [14]. For the small 1T atom cluster, the PA equals 1330 kJ/mol [14]. These results agree with the experimentally measured proton affinities for HZSM5, which are in the range 1190–1330 kJ/mol [42]. The difference in proton affinity for the various clusters is one of the reasons for the few kilojoules difference in the activation barriers or adsorption energies observed using different clusters models for the zeolite. Although most of the properties are convergent with increasing cluster size, the proton affinity mostly oscillates or very slowly converges with increasing cluster size [39,40]. At present there is no "perfect" cluster model for the zeolite, but all have their intrinsic advantages and disadvantages. Since the computational time of calculation increases dramatically with increasing cluster size a compromise between (i) size of the system, (ii) computer expenses, and (iii) desired accuracy has to be made for each system individually.

6. Mechanistic study of reaction paths for chemical reactions

With the increasing understanding of the microscopic interaction of guest molecules with the zeolitic lattice, the mechanistic study of chemical reactions starts to become possible. We will analyze the dimethyl ether formation, one of the steps in the MTG (methanol to gasoline) process [43], which is one of the most successful routes for the catalytic conversion of methanol to hydrocarbons in the gasoline boiling range (30–200°C). A large variety of different experiments established that methanol catalyzed by an acidic zeolite is first dehydrated to dimethyl ether (DME) [44] and that an equilibrium mixture of methanol and DME is then converted to olefins, aliphatics and aromatics up to C_{10}. The mechanism of methanol adsorption at low and high coverages [12,14] and, especially, the dehydration reaction path to DME has recently been presented for the first time [12,14,45]. One of the most accepted mechanisms for DME formation [46] proposed that two distinct steps are necessary for the formation of DME. First one methanol molecule is dehydrated leaving a methyl group bonded to the zeolitic surface, the surface methoxy species discussed in section 3 [12]. In a consecutive step those surface methoxy groups can react with another methanol molecule to form dimethyl ether. Such a mechanism has been recently studied by means of DFT theory [14,45]. The two (important) transition states for this reaction are shown in figs. 5a and 5b. The first is associated with the dehydration of the first methanol molecule and the second the interaction of the second methanol molecule with the methoxy surface resulting in the DME formation. Comparing the activation barriers for each step (taken with respect to the most stable mode of adsorption of the reactants or true barrier), 215 and 160 kJ/mol, one concludes that the dehydration process is over 50 kJ/mol more difficult than the DME formation. The first (dehydration) is, thus, the limiting step of the reaction.

Additionally, an alternative path for DME formation via an associative mechanism has also been presented [14,45]. According to this mechanism, from the association of two methanol molecules adsorbed simultaneously at the acidic and basic sites of the zeolite, DME

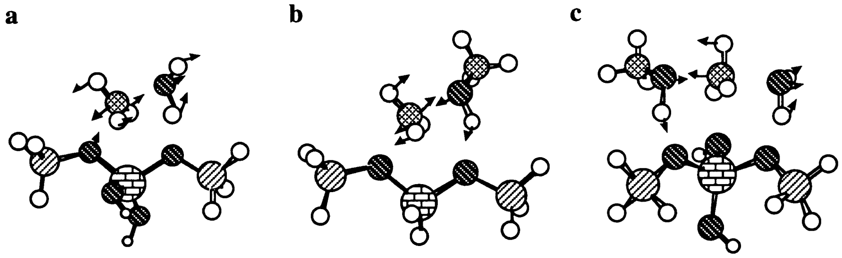

Fig. 7. Transition states for (a) methanol dehydration, (b) dimethyl ether formation via a surface methoxy species, and (c) simultaneous dehydration and dimethyl ether formation according to an associative mechanism. See fig. 1 for the pattern of the atoms. (Picture (a) is reprinted from ref. [12], copyright 1995 American Chemical Society; and pictures (b) and (c) are from ref. [45].)

and water can be formed in one step. The transition state involved is shown in fig. 7c. The activation barrier with respect to reactants in the gas phase (the apparent activation barrier) is only 15 kJ/mol. The reason for such a low barrier is very probably the fact that the trigonal planar carbenium-like part, in the center of the transition state (see fig. 7c), is now being stabilized not only by lattice but also by the almost formed water molecule at the right-side as well as by the methanol molecule at the left-side. The true activation barrier for DME formation according to this associative mechanism, 145 kJ/mol, is 70 kJ/mol lower than the limiting step for DME formation via the methoxy surface. An associative mechanism is, thus, the preferred route for DME formation [45].

7. Conclusions

A detailed microscopic understanding of the mechanism of zeolite Brønsted-acid catalyzed reactions introduced a new concept for protonated intermediates in solid acid catalysis, in terms of transition states closely interacting with the zeolitic lattice.

Very important in the zeolite acid catalyzed reactions is not only the acidic proton itself but also the presence of strong Lewis-basic oxygen atoms that are able to help in the stabilization of carbocation-like structures adsorbed at the surface. They are able to accommodate alkoxy groups generated from explicit protonation followed by cracking reactions as well as to auxiliate the C–C or C–O bond formation by helping also a back-donation of the proton from the molecular system to the zeolitic lattice, regenerating the acidic site.

With respect to the nature of the carbenium-like transition state formed, secondary and tertiary carbenium-like ions are more stable than primary and, especially, much more stable than the CH_3^+ groups. Thus, the last require stronger stabilization from the lattice than the first two. The difference in stability of the various carbenium ions is reflected in differences of the activation barriers, which are much higher for reactants like ethane than for isobutane.

According to the geometry of the transition state formed (distances of the carbocation-like formed from the surface), it can be considered more covalent (hydrogen deuterium exchange reactions) or more ionic (dehydrogenation or cracking reactions) in nature. The transition states that have a more covalent character are more sensitive to the influences of structural changes in the zeolite, while more ionic transition states are less affected by it.

Different overall reaction mechanisms can be theoretically studied. For methanol conversion a consecutive mechanism involving formation of an intermediate surface methoxy species appears to be unfavorable when compared to an associative bimolecular mechanism. Since a more stable transition state is involved the activation barrier involved is lower and the reaction via an associative mechanism is, thus, easier.

Acknowledgement

SRB thanks CNPq (Brazil) for a scholarship. Computational resources are supplied by the NCF (The Netherlands) under projects SC-183 and SC-417.

References

[1] G.J. Kramer, A.J.M de Man and R.A. van Santen, J. Am. Chem. Soc. 113 (1991) 6435.

[2] G.V. Gibbs, Am. Mineral. 67 (1982) 421.

[3] H. van Bekkum, E.M. Flanigen and J.C. Jansen, eds., *Introduction to Zeolite Science and Practice*, Studies in Surface Science and Catalysis, Vol. 58 (Elsevier, Amsterdam, 1991) chs. 12, 15.

[4] G.A. Olah, G.K.S. Prahash and J. Sommer, in: *Superacids* (Wiley, New York, 1985).

[5] G.J. Kramer and R.A. van Santen, Chem. Rev. 95 (1995) 637.

[6] W.J. Hehre, L. Radom, P. von R. Schleyer and J.A. Pople, in: *Ab Initio Molecular Orbital Theory* (Wiley, New York, 1986) chs. 12, 15.

[7] F.G. Oliver, E.J. Munson and J.F. Haw, J. Phys. Chem. 96 (1992) 8106;
E.J. Munson, A.A. Kheir, N.D. Lazo and J.F. Haw, J. Phys. Chem. 96 (1996) 7740;
E.J. Munson and J.F. Haw, J. Am. Chem. Soc. 113 (1992) 6303.

[8] J.A. Lercher, R.A. van Santen and H. Vinek, Catal. Lett. 27 (1994) 91.

[9] S.R. Blaszkowski, A.P.J. Jansen, M.A.C. Nascimento and R.A. van Santen, J. Phys. Chem 98 (1994) 12938.

[10] G.J. Kramer and R.A. van Santen, J. Am. Chem. Soc. 115 (1993) 2889.
[11] F. Haase and J. Sauer, J. Am. Chem. Soc. 117 (1995) 3780.
[12] S.R. Blaszkowski and R.A. van Santen, J. Phys. Chem. 99 (1995) 11728.
[13] C.M. Zicovich-Wilson, P. Viruela and A. Corma, J. Phys. Chem. 99 (1995) 13224.
[14] S.R. Blaszkowski and R.A. van Santen, submitted.
[15] M. Krossner and J. Sauer, J. Phys. Chem. 100 (1996) 6199;
J. Sauer, Science 271 (1996) 774.
[16] L. Smith, A.K. Cheetam, R.E. Morris, L. Marchese, J.M. Thomas, P.A. Wright and J. Chen, Science 271 (1996) 799.
[17] S.J. Collins and P.J. O'Malley, J. Catal. 153 (1995) 94.
[18] V.B. Kazansky, I.N. Senchenya, M. Frash and R.A. van Santen, Catal. Lett. 27 (1994) 345.
[19] S.R. Blaszkowski, M.A.C. Nascimento and R.A. van Santen, J. Phys. Chem. 100 (1996) 3463.
[20] V.B. Kazansky, M. Frash and R.A. van Santen, Appl. Catal. A 146 (1996) 225.
[21] V.B. Kazansky and I.N. Senchenya, J. Mol. Catal. 74 (1992) 257;
V.B. Kazansky, Acc. Chem. Res. 24 (1991) 379;
V.B. Kazansky and I.N. Senchenya, J. Catal. 119 (1989) 108.
[22] G.J. Kramer, R.A. van Santen, C.A. Emeis and A.K. Novak, Nature 363 (1993) 529.
[23] P. Viruela-Martín, C.M. Zicovich-Wilson and A. Corma, J. Phys. Chem. 97 (1993) 13713.
[24] D.K. Bohme, in: *Interactions between Ions and Molecules*, ed. P. Ausloos (Plenum Press, New York, 1975).
[25] L. Kubelková, J. Nováková and P. Jíru, in: *Structure and Reactivity of Modified Zeolites*, eds. P.A. Jacobs et al. (Elsevier, Amsterdam, 1984);
J. Nováková, L. Kubelková and Z. Dolejsek, J. Catal. 108 (1987) 208;
J. Nováková, L. Kubelková and Z. Dolejsek, J. Mol. Catal. 45 (1988) 365.
[26] V.B. Kazansky, M. Frash and R.A. van Santen, in: *Proc. 11th Int. Zeolite Conf.*, Seoul 1996, to be published.
[27] V.B. Kazansky, M. Frash and R.A. van Santen, Catal. Lett. 28 (1994) 211.
[28] V.B. Kazansky, M. Frash and R.A. van Santen, in: *Proc. 11th Int. Congr. of Catalysis – 40th Anniversary*, eds. J.W. Hightower, W.N. Delgass, E. Iglesia and A.T. Bell (Elsevier, Amsterdam, 1996) p. 1233.
[29] E.M. Evleth, E. Kassab and L.R. Sierra, J. Phys. Chem. 98 (1994) 1421.P.
[30] G.J. Kramer and R.A. van Santen, J. Am. Chem. Soc. 117 (1995) 1766.
[31] H. Krannila, W.O. Haag and B.C. Gates, J. Catal. 135 (1992) 115.
[32] A. Corma, P.J. Miguel and A.V. Orchillés, J. Catal. 145 (1994) 58.
[33] S.P. Bates, W.J.M. van Well, R.A. van Santen and B. Smit, J. Am. Chem. Soc. 118 (1996) 6753.
[34] T.F. Narbeshuher, PhD Thesis, University of Twente, The Netherlands (1994) ch. 4;
A. van de Runstraat, P.J. Stobbelaar, J. van Grondelle, B.G. Anderson, L.J. van IJzendoorn and R.A. van Santen, *Proc. 11th Int. Zeolite Conf.*, Seoul 1996, to be published.
[35] L.W. Beck, T. Xu, J.B. Nicholas and J.F. Haw, J. Am. Chem. Soc. 117 (1995) 11594.
[36] R.A. van Sante, B.W.H. van Beest and A.J.M. de Man, in: *Guidelines for Mastering the Properties of Molecular Sieves*, NATO ASI Series B, Vol. 221, eds. D. Barthomeuf, E.G. Derouane and W. Höelderich (Plenum, Amsterdam, 1990) p. 227.
[37] R. Shah, M.C. Payne, M.-H. Lee and J.D. Gale, Science 271 (1996) 1395.
[38] L. Limtrakul, Chem. Phys. 193 (1995) 79.
[39] H.V. Brand, L.H. Curtiss and L.E. Iton, J. Phys. Chem. 96 (1992) 7725; 97 (1993) 12773.
[40] M.S. Stave and J.B. Nicholas, J. Phys. Chem. 97 (1993) 9630; 99 (1995) 15046.
[41] J. Sauer, J. Mol. Catal. 54 (1989) 312;
P.J. O'Malley and J. Dwyer, Chem. Phys. Lett. 143 (1988) 97; J. Phys. Chem. 92 (1988) 3005;
J.B. Nicholas, R.E. Winans, R.J. Harrison, L.E. Iton, L.A. Curtiss and A.J. Hopfinger, J. Phys. Chem. 96 (1992) 10247;
A.E. Alvarado-Swaisgood, M.K. Barr, P.J. Hay and A. Redondo, J. Phys. Chem. 95 (1991) 10031;
J.C. White and A.C. Hess, J. Phys. Chem. 97 (1993) 6398, 8703.
[42] J. Datka, M. Boczar and P. Rymarowicz, J. Catal. 114 (1988) 368.
[43] S.L. Meisel, J.P. McCullogh, C.H. Lechthaler and P.B. Weisz, CHEMTECH 6 (1976) 86;
C.D. Chang, in: *Hydrocarbons from Methanol* (Dekker, New York, 1983).
[44] J.J. Spivey, Chem. Eng. Comm. 110 (1991) 123.
[45] S.R. Blaszkowski and R.A. van Santen, J. Am. Chem. Soc. 118 (1996) 5152;
S.R. Blaszkowski and R.A. van Santen, in: *Proc. 11th Int. Zeolite Conf.*, Seoul 1996, to be published.
[46] L. Kubelková, J. Nováková and K. Nedomová, J. Catal. 124 (1990) 441.